Hindawi
Wireless Communications and Mobile Computing
Volume 2020, Article ID 8898672, 15 pages
https://doi.org/10.1155/2020/8898672

Research Article

Evaluation of Localization by Extended Kalman Filter, Unscented Kalman Filter, and Particle Filter-Based Techniques

Inam Ullah,[1] Xin Su,[1] Jinxiu Zhu,[1] Xuewu Zhang,[1] Dongmin Choi,[2] and Zhenguo Hou[3]

[1]*College of Internet of Things (IoT) Engineering, Hohai University (HHU), Changzhou Campus, 213022, China*
[2]*Division of Undeclared Majors, Chosun University, Gwangju 61452, Republic of Korea*
[3]*China Construction Seventh Engineering Division CoRP, Ltd, 108 Chengdong Road, Jinshui District, Zhengzhou City, Henan Province, China*

Correspondence should be addressed to Dongmin Choi; jdmcc@chosun.ac.kr

Received 13 June 2020; Revised 10 August 2020; Accepted 17 September 2020; Published 5 October 2020

Academic Editor: Changqing Luo

Mobile robot localization has attracted substantial consideration from the scientists during the last two decades. Mobile robot localization is the basics of successful navigation in a mobile network. Localization plays a key role to attain a high accuracy in mobile robot localization and robustness in vehicular localization. For this purpose, a mobile robot localization technique is evaluated to accomplish a high accuracy. This paper provides the performance evaluation of three localization techniques named Extended Kalman Filter (EKF), Unscented Kalman Filter (UKF), and Particle Filter (PF). In this work, three localization techniques are proposed. The performance of these three localization techniques is evaluated and analyzed while considering various aspects of localization. These aspects include localization coverage, time consumption, and velocity. The abovementioned localization techniques present a good accuracy and sound performance compared to other techniques.

1. Introduction

Accurate localization is a very important aspect of several wireless sensor networks (WSNs) and Internet of Things (IoT) applications. These applications included underwater navigation, indoor positioning, bridges monitoring, industrial monitoring, health monitoring, and security systems [1–4]. For the improvement of localization accuracy, a variety of localization techniques have been investigated in the previous work. However, in this paper, the authors focused on three basic localization techniques named Extended Kalman Filter (EKF-) based localization, Unscented Kalman Filter (UKF-) based localization, and Particle Filter (PF-) based localization.

In the early period, Kalman Filter (KF) is used in an iterative manner that considers the prior information of the noise features to compensate for and to filter out the noise. But still, the issues arise during localization when attempting to model the noise that is only an approximation and does not specify the noise real distribution [5–7]. KF is only applicable for the linear stochastic procedures; however, for the nonlinear procedures, the EKF can be applied. The supposition of these two methods (KF and EKF) is that noise and process measurements are self-governing and with a normal probability distribution [8].

The authors analyzed the pertinency of the KF to the mobile robot self-positioning in [9–11]. These algorithms are only appropriate for linear systems. On the other hand, for robot self-positioning, EKF provides an alternative to the Bayesian filter. Therefore, in [12], the author proposed an EKF approach for the localization of four-wheel encoders and laser range-finder nodes. EKF is basically used for the nonlinear functions, which apply the Taylor series expansion to linearize the measurement models. Thus, the first-order nonlinear functions of the Taylor series is used. In the predictable statistics of the subsequent distributions, this linearization often encourages higher error. This is particularly obvious when the systems are vastly nonlinear, and it can lead to the deviation in the filter. Besides, the UKF does not estimate the nonlinear method, and the actual nonlinear

model is applied to the observation models. UKF basically estimate the distribution of random variables [13] by applying the scaled unscented alteration method. For the autonomous robot localization or Autonomous Underwater Vehicles (AUV) localization, the EKF and UKF performance is equated in [14]. The author concludes that the UKF performance is better concerning numerous characteristics such as average localization accuracy relative to the EKF. Besides this, UKF does not involve applying the Jacobian matrix; therefore, the UKF precision is higher.

The PFs have taken further consideration by the investigators because of their advantages against the EKF and the UKF [15]. PF can solve the issue of a measurement system that is affected by the non-Gaussian noise and accomplish the localization globally in the case in which there is no prior knowledge about the target [16]. The PFs are easier in implementation as compared to the EKF, but also exist some disadvantages such as letdown due to sample penury and substantial computational load. The letdown due to the sample penury occur more commonly and resultantly causes the failure of the PF algorithm. To address this issue, various PFs have been investigated such as Markov Chain Monte Carlo (MCMC) move step and Regularized PF (RPF) [17]. The proposed approaches cannot prevent it completely but can mitigate the sample penury. If the conventional PF flops because of the sample penury, it is unable to return to the normal conditions. Furthermore, a Hybrid Particle/Finite Impulse Response (FIR) Filter (HPFF) is investigated to solve this issue [18–21]. FIR filters are more stable as compared to other filters and robust, but FIR filters characteristically drop inaccuracy to the PF in the case of nonlinear systems [22–25]. Therefore, PF is applied as an elementary filter, which is susceptible to failure and deviation. The FIR filter is applied to recuperate the PF by restarting and reorganizing.

1.1. Contributions of This Work. This work aims to propose an effective vehicular localization technique for the mobile robot. For this purpose, the authors introduced three localization techniques. The proposed techniques' performance is better in simulation concerning the abovementioned localization techniques in the literature. The contributions of this paper are divided into the following three phases.

(1) EKF-based localization

(2) UKF-based localization

(3) PF-based localization

The performance of the abovementioned techniques is evaluated and analyzed in different scenarios. While considering numerous aspects of localization, the accuracy of these techniques is higher. A variety of vehicular localization techniques are investigated in the literature to analyze the presentation of the proposed techniques. These techniques are evaluated while considering numerous aspects of localization such as accuracy, time consumption, vehicle velocity, coverage area, and localization coverage. Furthermore, the presentation of the proposed localization techniques is compared with each other's and also with other localization techniques.

1.2. Organization. The rest of the paper is sorted as follows. The related work is detailed in Section 2, and Section 3 presents the proposed techniques used for localization. The subsections of Section 3 present the proposed EKF, UKF, and PF localization techniques. Section 4 presents the discussion on the simulation results and comparison while Section 5 concludes the work.

2. Related Work

In order to expand the performance of mobile robot localization, several approaches have been introduced [26–28] to address vehicular localization [29] issues and errors of the NLoS environment. The method in [30] uses two receivers, and the Frequency Difference of Arrival (FDoA) signals to approximate the moving emitter velocity. There is a nonlinear measurement error which is occurred by the RF system noise in the geolocation environment with the Time Difference of Arrival (TDoA) [31, 32] and FDoA. For this problem, the authors proposed the iterated dual-EKF approach to recompense for the nonlinear estimation error. Using the iterated dual-EKF approach, the parameter estimation (PE) filter updates model uncertainties caused by exterior noises and has a higher convergence rate of the system parameters by the iteration method.

EKF is a traditional technique for positioning estimation [33, 34]. EKF extends models of nonlinear functions in the Taylor series close to the estimation state and shortens them to consider the linearization of the model in the first order. In the Line-of-Sight (LoS) environment, EKF based on the linear models achieves higher accuracy. But, if the channel is in the NLoS environment, the EKF shows a high error in localization because of measurement data deviation [35]. For mobile node localization, a variety of NLoS approaches have been presented [36–40]. The method of unscented transformation is used for the standard KF to produce the UKF, which attains a better estimation than the other methods. Another method is presented for the positioning of targets named Adaptive Iterated Unscented KF (AIUKF) which combines the adaptive factor and iterative approach to improve the localization performance. A PF localization approach based on the Monte Carlo technique is used for the positioning which exploits random sample group information for the approximation of the state Probability Density Function (PDF). Therefore, the performance of the PF-based localization in non-Gaussian is much better while demanding a high number of sample points. The authors collected all metrics of the range and obtained the final estimation of the state on the basis of position estimation of the fusion subgroup. But on the other hand, in the NLoS, the authors find discarding and detecting the range calculation from the beacon nodes. However, most of the above methods perform accurately only in a particular noise distribution field, which is not authentic.

Perhaps, EKF is a well-known procedure for estimating a noisy measurement of the nonlinear system state. EKF is based on the nonlinear maps of the system around the estimated route. It is also based on the idea that the noises of measurement, input noise, and initial state are Gaussian. It

is acknowledged that the EKF is likely to deviate, mostly because of bad primary estimates and higher noises, but our experience does not know of any testable convergence conditions. The estimation divergence is extra probable when measurements are lost due to communication faults [41, 42], which is a communal disorder in mobile robotics.

In recent years, UKF was developed to tackle some problems such as the need for Gaussian noises and the properties of poor approximation [43]. The basic idea of UKF is to find a transformation that allows a random vector having a length of n to approximate the covariance and mean when it is changed by the nonlinear map. It can be achieved by calculating a set of $2n + 1$ points, known as σ-points, based on the innovative vector mean and variance, transforming those points through the nonlinear map and then resembling the transformed vector mean and variance from the transformed σ-points. The authors investigated that the EKF estimate is precise to the first order, while in the case of Gaussian noises, the UKF is precise to the third order. Similarly, for the EKF, the covariance of the estimate is precise to the first order and second order for the UKF.

A procedure of tracking through PFs is presented in [44] to produce a probability distribution over the targeted area. The procedure applies the recursive Bayesian filters which are based on the sequential MC technique of sampling to estimate the location of the target posterior distribution by applying another distribution that can be prior arbitrary. PF begins with a regularly primed set of particles. Then, according to a movement model, all particle positions are modified. The authors considered the measure in the (x, y) space that follows an arbitrary walk model for the representation of the human movement. The $x(t + \tau) = x(t) + \varphi(\tau)$ shows a random path of the user, where φ denotes the random parameter which characterizes the probability of following a known direction in the tracking procedure next phase. In the measures achieved from the tags deployed in RFID, the model also takes into consideration the error model.

A statistical method named Kullback-Leibler Distance (KLD) sampling is presented to increase the efficiency of the PFs by adapting the sample sets size on-the-fly [45]. The approach is used to link the error of approximation which is introduced by the PF sample-based illustration. The method selects a smaller number of samples if the density is observant to a small part of the state space, and rising samples if the uncertainty of the state is high. The mobile robot localization problem is used to test and demonstrate the approach to the adaptive PF. The localization of robots is the problem of estimating the position of a robot relative to the map of its operation area. This issue has been identified as one of the most important mobile robotics challenges which come in diverse essences. The simplest problem with localization is position tracking, where the primary location of the robot is determined, and location pursues to exact small, gradual errors in the robot's odometry. The global localization is another stimulating problem for mobile robots, where a robot does not have prior knowledge about his position, but it has to be decided from scratch, instead.

Following the above discussion, it is reflected that to present efficient and accurate localization techniques, the issue of vehicular localization with limited features is previously important. Most of the previous localization techniques focused only on the vehicle localization accuracy while ignoring several aspects such the vehicle velocity, time consumption, and coverage. Besides this, we must take into account the positioning of the mobile robot in a precise manner. The author, therefore, considers three localization techniques named EKF, UKF, and PF in this paper. The proposed techniques are evaluated on the basis of their performances. The authors consider several aspects for localization such the vehicle velocity, time consumption, accuracy, and localization coverage.

3. Proposed Techniques of Localization

This section discusses the proposed localization techniques based on EKF, UKF, and PF. In the next pages, the proposed localization techniques are examined. Table 1 shows the notations used in this work.

3.1. Extended Kalman Filter-Based Localization. EKF is typically implemented by substitution of the KF for nonlinear systems and noise models. The models of observation and state transformation are nonlinear functions, but these can be differentiable functions. The observation and state transition models [46] are delineated as

$$x_k = f(x_{k-1}, u_k) + w_k, \tag{1}$$

$$z_k = h(x_k) + v_k. \tag{2}$$

In the above equations, w_k and v_k denote the process and observation noises and zero-mean Gaussian with the covariance Q_k and R_k, where x_k and x_{k-1} are the current and previous robot state, while u_k represents the input vector.

The state covariance is calculated as

$$P_k = \begin{bmatrix} P_{x_v} & P_{x_v l} \\ P_{l x_v} & P_{ll} \end{bmatrix} = \begin{bmatrix} P_{x_v x_v} & P_{x_v l_1} & \cdots & P_{x_v l_1} \\ P_{l_1 x_v} & P_{l_1 l_1} & \cdots & P_{l_1 l_n} \\ \cdots & \cdots & \cdots & \cdots \\ P_{l_n x_v} & \cdots & \cdots & P_{l_n l_n} \end{bmatrix}, \tag{3}$$

where P_k is the covariance of the estimated $n \times n$ matrix. Prediction and update states are the two stages of the EKF algorithm. To calculate the prediction state

$$\widehat{x}_{k|k-1} = F \times \widehat{x}_{k-1|k-1} + B_k \times u_k, \tag{4}$$

where F denotes the state transition and B_k denotes the input matrix. Covariance from equation (3) will become

$$P_{k|k-1} = F \times P_{k-1|k-1} \times F^T + Q, \tag{5}$$

where $P_{k|k-1}$ and $P_{k-1|k-1}$ are the current and previous states. Q represents a covariance matrix for the noise process. The

Table 1: Index of notation.

Notation	Description
T	Time interval
φ	Random parameter
X_k	Current state
X_{k-1}	Previous state
Z_k	Observation model
f	Prediction state function
h	Prediction measurement function
$P_{k/k-1}$	Current state covariance
$P_{k-1/k-1}$	Previous state covariance
Q	Covariance matrix of the process noise
R	Covariance matrix of the measurement noise
$h(\widehat{X}_k)$	Predictable estimation
S_k	Covariance matrix of $\tilde{y}_k$
H_k	Predictable estimation Jacobian matrix
K_k	Kalman optimal gain
$P_{k/k}$	Covariance matrix subsequent state
$F\&B$	State transition matrices
δ_x^2	Standard deviation
x, y	Denote locations
$P_\circ$	State information vector
H	Output measurement matrix
v_{k-1}	Process noise
n_k	Measurement noise
w	Weights
$x_\circ$	Sigma point
x_i	Sigma point where $i = 1, 2, \cdots, 2n$
x_{est}	Estimation state
x_{tru}	True state
n	Dimension of x
s_k	Set of particles
$p(2k/x_k^i)$	Importance factor
$f_k(x_k)$	Positive state function
T_s	Robot sampling time
$p(x_k/z_1 : k)$	Successive approximation
$\delta(.)$	Dirac function
N	Denote the samples

origination vector and covariance matrix for the EKF update state is

$$\begin{aligned} \tilde{Y}_k &= Z_k - h(\widehat{X}_k), \\ S_k &= H_k \times P_{k|k-1} \times H_k^T + R_k, \end{aligned} \tag{6}$$

where $h(\widehat{X}_k)$ is the predictable estimations, S_k denotes the covariance matrix of $\tilde{Y}_k$, and H_k is the predictable estimations Jacobian matrix. To calculate the subsequent state vector:

$$\begin{aligned} \widehat{x}_{k|k} &= \widehat{X}_{k|k-1} + K_k \times \tilde{Y}_k. \\ K_k &= P_{k|k-1} \times H_k^T \times S_k^{-1}, \\ P_{k|k} &= (I_n - K_k \times H_k) \times P_{k|k-1}, \end{aligned} \tag{7}$$

where K_k is the Kalman optimal gain and $P_{k|k}$ denotes the covariance matrix subsequent state. To apply the prediction, motion, and observation models, the state vector is computed as

$$X_k = [x\, y\, \text{yaw}\, v]^T. \tag{8}$$

Therefore, the state transition matrices F and B are calculated as

$$\begin{aligned} F &= \begin{bmatrix} 1 & 0 & 0 & 0 \\ 0 & 1 & 0 & 0 \\ 0 & 0 & 1 & 0 \\ 0 & 0 & 0 & 0 \end{bmatrix}, \\ B &= \begin{bmatrix} dt.\cos(x(3)) & 0 \\ dt.\sin(x(3)) & 0 \\ 0 & dt \\ 1 & 0 \end{bmatrix}, \end{aligned} \tag{9}$$

In the same way, the measurement noise R is calculated as

$$R = \begin{bmatrix} \cos(\theta) & \sin(\theta) \\ -\sin(\theta) & \cos(\theta) \end{bmatrix}. \tag{10}$$

The Jacobian of the measuring system's motion model and covariance can be computed as

$$\begin{aligned} \text{JF} &= \begin{bmatrix} 1 & 0 & 0 & 0 \\ 0 & 1 & 0 & 0 \\ -dt.\sin(x(3)) & dt.u(1).dt.\cos(x(3)) & 1 & 0 \\ dt.\cos(x(3)) & dt.\sin(x(3)) & 0 & 1 \end{bmatrix}, \\ P_0 &= \begin{bmatrix} \sigma_x^2 & 0 & 0 & 0 \\ 0 & \sigma_y^2 & 0 & 0 \\ 0 & 0 & \sigma_{vx}^2 & 0 \\ 0 & 0 & 0 & \sigma_{vy}^2 \end{bmatrix}, \end{aligned} \tag{11}$$

where σ_x^2 denotes the standard deviations of the estimated x, y locations and P_0 is the state information vector. The value of

the standard deviation, in this case, depends on certain variables such as the accuracy of GPS and the distance as shown in Figure 1. Thus, the measuring system Jacobian can be written as

$$H = \begin{bmatrix} 1 & 0 & 0 & 0 \\ 0 & 1 & 0 & 0 \\ 0 & 0 & 1 & 0 \\ 0 & 0 & 0 & 1 \end{bmatrix}, \tag{12}$$

where H is the output measurement matrix and the Jacobian matrices of the state equation. The localization results of the EKF algorithm is shown in Figure 1.

3.2. Unscented Kalman Filter-Based Localization. UKF is a nonderivative filtering approach that immediately propagates the mean measurement covariance and the state estimates. Therefore, it precisely represents the allied distributions by any nonlinear transformations that include the measurement and state dynamics. In the process model, because of the nonlinearity in the state functions of the velocity, unscented approximation to the finest filtering explanation can be derived by implementing two steps of measurement and time update. In the implementation of the two phases, an unscented transform is approved for the sigma points formation. Furthermore, for the derivation of UKF, the Jacobian matrix calculation is not required as required for the EKF technique. The technique can proceed in the following way. Provided a nonlinear system with a discrete time-system model [47, 48]:

$$\begin{aligned} x_k &= f(x_{k-1}, v_k, u_{k-1}), \\ y_k &= h(x_k, n_k, u_k), \end{aligned} \tag{13}$$

where v_{k-1} and n_k show the process noise and measurement noise. Further, to compute the sigma points, time, and measurement update, the x_k estimates can be calculated. A set of test points and its related weights w at time $k-1$ is utilized for sigma points measurement such as $x_0, k-1 = x_{k-1}$, where x_0 denotes the sigma point at state:

$$x_{\text{est}} = \begin{bmatrix} 0 & 0 & 0 & 0 \end{bmatrix}^T, \tag{14}$$

where x_{est} is the estimated state. The state will be true if $x_{\text{tru}} = x_{\text{est}}$. The corresponding weights for the sigma points can be calculated as

$$\begin{aligned} x_{i,k-1} &= x'_{k-1} + \left[\sqrt{(n+\lambda) \times P_{k-1}}\right]_i, \\ x_{i,k-1} &= x'_{k-1} - \left[\sqrt{(n+\lambda) \times P_{k-1}}\right]_{i-n}, \end{aligned} \tag{15}$$

where x_i denotes the sigma points and $i = 1, 2, \cdots, 2n$. Normally, the weights w are characterized as

$$\begin{aligned} w^m &= \left[\frac{\lambda}{n+\lambda}\right], \\ w^c &= \left[\left(\frac{\lambda}{n+\lambda}\right) + \left(1 - \alpha^2 + \beta\right)\right]. \end{aligned} \tag{16}$$

Similarly, at $t = 0$, the weights w^m and w^c can be written as

$$\begin{aligned} w_0^m &= \left[\frac{\lambda}{n+\lambda}\right], \\ w_0^c &= \frac{\lambda}{(n+\lambda) + (1 - \alpha^2 + \beta)}, \\ w_i^m &= w_i^c = \frac{1}{2(n+\lambda)}, \end{aligned} \tag{17}$$

where the dimension of x represented by n and $\lambda = \alpha^2(n + k) - n$ is the parameter of scaling. Moreover, α is applied to find the sigma points spreading around the state variable x' mean, and k is the second scaling parameter. To compute the prediction of sigma points with observation and motion model, the covariance and mean will become

$$\begin{aligned} x_{i,k|k-1} &= f(x_{i,k-1}), \\ \bar{x}' &= \sum_{i=0}^{2n} w_i^m x_{i,k|k-1}, \\ p'_k &= \sum_{i=0}^{2n} w_i^c \left[x_{i,k|k-1} - \bar{x}'\right]\left[x_{i,k|k-1} - \bar{x}'\right]^T + Q_k, \\ \dot{x}_{i,k|k-1} &= \left[x_{0:2n,k|k-1} \quad x_{0,k|k-1} + \nu\sqrt{Q_k} \quad x_{0,k|k-1} - \nu\sqrt{Q_k}\right]_i. \end{aligned} \tag{18}$$

With supplementary points gained from the process noise covariance matrix square root, the sigma points were increased.

$$\begin{aligned} \dot{y}_{i,k|k-1} &= h\left(\dot{x}_{i,k|k-1}\right), \\ \bar{y}' &= \sum_{i=0}^{2n^a} \dot{w}_i^m \dot{Y}_{i,k|k-1}, \\ p_{yy,k} &= \sum_{i=0}^{2n^a} \dot{w}_i^c \left[\dot{Y}_{i,k|k-1} - \bar{y}'_k\right]\left[\dot{Y}_{i,k|k-1} - \bar{y}'_k\right]^T + R_k, \\ p_{xy,k} &= \sum_{i=0}^{2n^a} \dot{w}_i^c \left[\dot{x}_{i,k|k-1} - \bar{x}'_k\right]\left[\dot{y}_{i,k|k-1} - \bar{y}'_k\right]^T, \end{aligned} \tag{19}$$

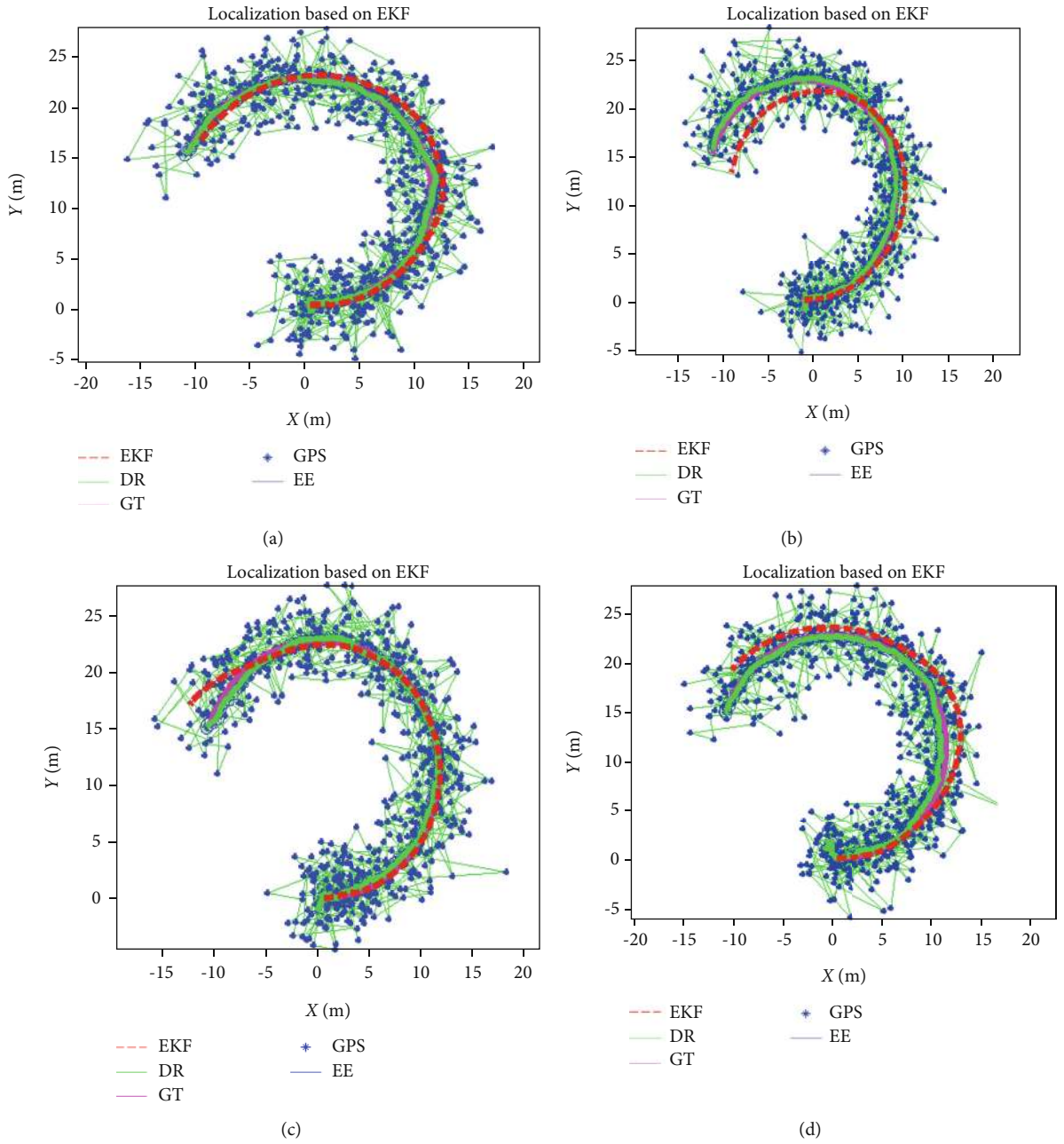

Figure 1: Localization comparison of EKF. In this phase, for all four iterations, the velocity is $v = 1$ m/s and time is $t = 60$ sec. In the legends, the red dashed line represents the EKF localization, where the green is the dead reckoning (DR), the pink solid line is the ground truth (GT), the blue color asterisks denote the GPS signals, and the blue line denotes the error ellipse (EE) during localization.

where R_k denote the covariance matrix. The Kalman gain can be computed to update the state and the covariance.

$$\begin{aligned} k_k &= p_{xy,k} \times p^{`1}_{yy,k}, \\ \bar{x}_k &= \bar{x}^{`} + k_k\left(y_k - \bar{y}^{`}\right), \\ p_k &= p^{`}_{k} - k_k \times p_{xy,k} \times k_k^T, \end{aligned} \tag{20}$$

By considering the primary estimation state, i.e., $x^{`}_0 = E[x_0]$ and $p_0 = E[(x_0 - x^{`}_0) \times (x_0 - x^{`}_0)^T]$

$$\begin{aligned} R &= \begin{bmatrix} \cos(\theta) & \sin(\theta) \\ -\sin(\theta) & \cos(\theta) \end{bmatrix}, \\ x_{k+1} &= Fx_k + Bv_k, \end{aligned} \tag{21}$$

where R denotes the covariance matrix for measuring noise and F and B can be calculated as

$$\begin{aligned} F &= \begin{bmatrix} 1 & 0 & 0 & 0 \\ 0 & 1 & 0 & 0 \\ 0 & 0 & 1 & 0 \\ 0 & 0 & 0 & 0 \end{bmatrix}, \\ B &= \begin{bmatrix} dt.\cos(x(3)) & 0 \\ dt.\sin(x(3)) & 0 \\ 0 & dt \\ 1 & 0 \end{bmatrix}, \\ H &= \begin{bmatrix} 1 & 0 & 0 & 0 \\ 0 & 1 & 0 & 0 \\ 0 & 0 & 1 & 0 \\ 0 & 0 & 0 & 1 \end{bmatrix}. \end{aligned} \tag{22}$$

In the above equations, F and B denote the state matrices of transition, while H represents the observation model output measurement matrix. The localization results of the UKF technique is presented in Figure 2.

3.3. Particle Filter-Based Localization. The authors analyzed the performance of the PF-based localization technique in this part. As similar to the tracking method, a PF is implemented to construct a probability distribution over the field of the targeted area of operation. This technique uses a recursive Bayesian filter based on the sampling of MC to calculate the target location subsequent distribution by applying another distribution which can be random a priori [40]. The PF approach is less intensive computationally in comparison to the EKF and UKF techniques. Besides this, in contrast to the KF, PF can avoid any supposition related to the intrinsic prominent attribute of the process and uncertainty related to the node information. The PF required an optimum interval of average but does not include the statistics on noise. Moreover, when the robot is traveling during the process of localization, the sensor particles in the surrounding of the robot can communicate with the robot and transfer information to the robot [45]. The mobile robot can receive a range of data from RFID that its position is known. The location of a robot in a regular PF can be defined by vector $x_k = [x_k \quad y_k]^t$. At the first step, the state estimation vector is $x_{\text{est}} = [0 \quad 0 \quad 0]^t$ with an estimate $\bar{x}_k$ of x_k. As mentioned in equations (1) and (2), the prediction and measurement models are calculated. Let's suppose, to describe a group of particles at instant k time:

$$\begin{aligned} s_k &= \left[\left(x_k^i, w_k^i\right) \mid i = 1, 2, 3, \cdots, n_s\right], \\ w_k^i &= \frac{p\left(x_k^i \mid z^k, u^k\right)}{p\left(x_k^i \mid u_k, x_{k-1}\right)p\left(x_{k-1} \mid z^{k-1}, u^{t-1}\right)}, \\ w_k^i &= \frac{\eta p\left(z^k \mid x_k^i\right)p\left(x_k^i \mid u_k, x_{k-1}\right)p\left(x_{k-1} \mid z^{k-1}, u^{k-1}\right)}{p\left(x_k^i \mid u_k, x_{k-1}\right)p\left(x_{k-1} \mid z^{k-1}, u^{k-1}\right)}, \\ w_k^i &= \eta p\left(z_k \mid x_k^i\right), \end{aligned} \tag{23}$$

where s_k is the set of particles, the numerator is the target distribution, and the denominator is the distribution proposal. Moreover, η is the constant and $p(z_k \mid x_k^i)$ denotes the importance factor. For the state function, $f_k(x_k)$ is supposed to be a positive function where the PF algorithm produces the samples from $f_k(x_k)p(x_k \mid z^k, u^k)$ where at the initial stage, the samples are at position $f_0(x_0)$.

To calculate the innovative samples, a random particle x_{k-1}^i is computed from X_{k-1} and being distributed for n in relation to $f_{k-1}(x_{k-1})p(x_{k-1} \mid z^{k-1}, u^{k-1})$. At state $x_k^i \sim p(x_k \mid u_k, x_{k-1}^i)$, the importance weights w can be written with the $f_k(x_k)$ function.

$$\begin{aligned} w_k^i &= \frac{f_k\left(x_k^i\right)p\left(x_k^i \mid z^k, u^k\right)}{f_{k-1}\left(x_{k-1}^i\right)p\left(x_k^i \mid u_k, x_{k-1}\right)p\left(x_{k-1} \mid z^{k-1}, u^{t-1}\right)}, \\ w_k^i &= \frac{f_k\left(x_k^i\right)\eta p\left(z^k \mid x_k^i\right)p\left(x_k^i \mid u_k, x_{k-1}\right)p\left(x_{k-1} \mid z^{k-1}, u^{k-1}\right)}{f_{k-1}\left(x_{k-1}^i\right)p\left(x_k^i \mid u_k, x_{k-1}\right)p\left(x_{k-1} \mid z^{k-1}, u^{k-1}\right)}. \end{aligned} \tag{24}$$

To replace the constant of proportionality, the above equation can be written as

$$w_k^i \propto p\left(z^k \mid x_k^i\right) \times \frac{f_k\left(x_k^i\right)}{f_{k-1}\left(x_{k-1}^i\right)}. \tag{25}$$

The particle motion can be anticipated at the time k by applying the particles that contain the robot position or location, such as $x_k^i = f(x_{k-1}^i) + w_k$.

$$x_k^i = x_{k-1}^i + \begin{bmatrix} v_k \times T_s \times \cos\theta_k \\ v_k \times T_s \times \sin\theta_k \end{bmatrix} + w_k. \tag{26}$$

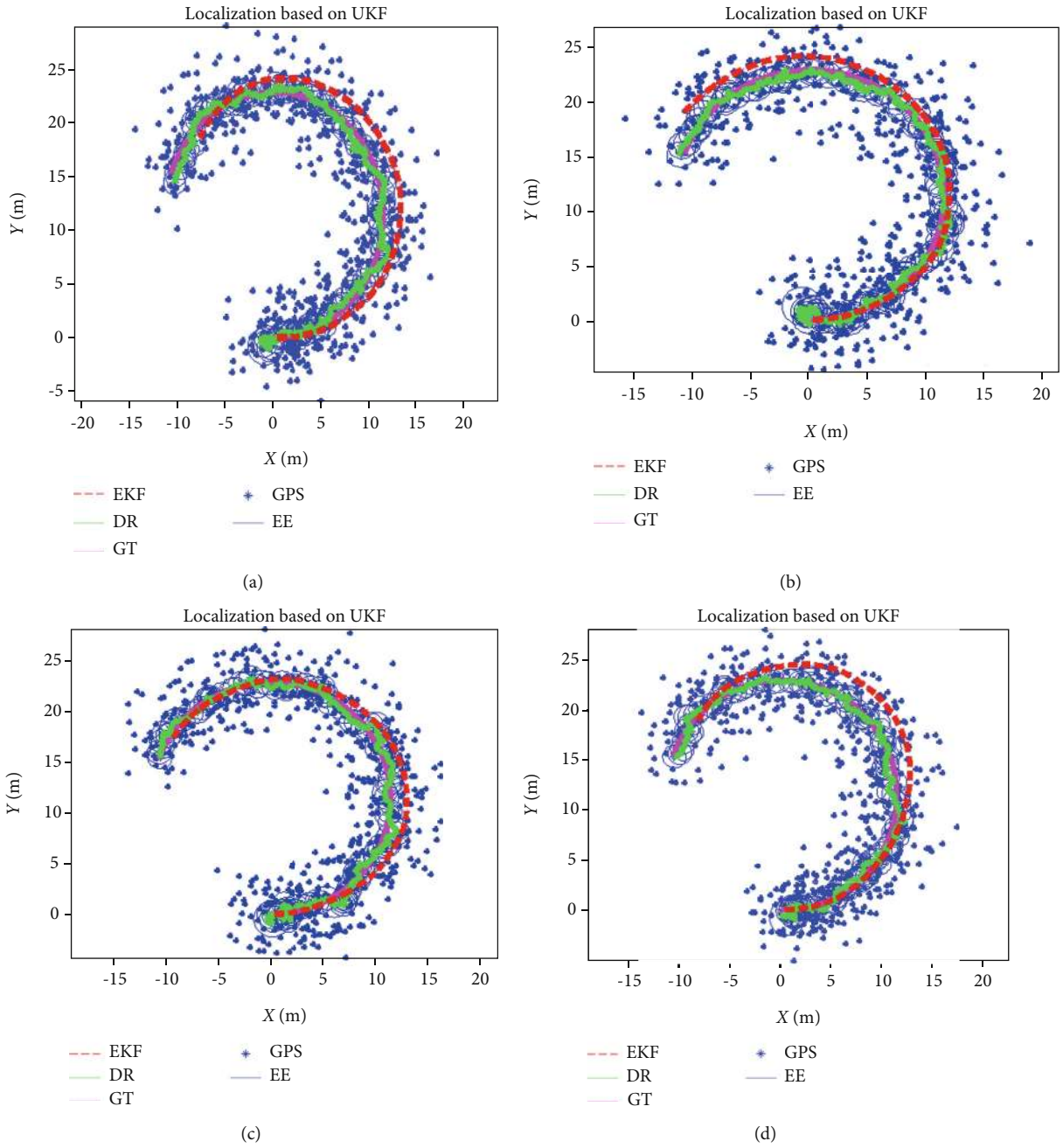

Figure 2: Localization comparison of UKF. In this phase, for all four iterations, the velocity is $v = 1$ m/s and time is $t = 60$ sec.

The state $\bar{x}_{k|k-1}$ estimate objectives can also be delineated by $\bar{x}_{k|k-1} = f(\bar{x}_{k-1|k-1})$.

$$p_{k|k-1} = \sum_{i=1}^{n_s} w_k^i \times \left[x_k^i - \bar{x}_{k|k-1}\right] \times \left[x_k^i - \bar{x}_{k|k-1}\right]^T + Q. \quad (27)$$

In the above equation, T_s is the robot sampling time, Q represents the covariance matrix, whereas the weight is represented by w. The successive approximation $p(x_k \mid z_{1:k})$ and the state $\bar{x}_{k|k}$ estimation can be calculated by:

$$p(x_k \mid z_{1:k}) \approx \sum_{i=1}^{N_s} w_k^i \times \delta\left(x_k - x_k^i\right), \quad (28)$$

$$\bar{x}_{k|k} = E[x_k \mid z_{1:k}], \quad (29)$$

$$\bar{x}_{k|k} = \int x_k \times p(x_k \mid z_{1:k}) dx_k \approx \sum_{i=1}^{N_s} w_k^i \times x_k^i, \tag{30}$$

$$p_{k|k} = \sum_{i=1}^{N_s} w_k^i \times \left[x_k^i - \bar{x}_{k|k}\right] \times \left[x_k^i - \bar{x}_{k|k}\right]^T, \tag{31}$$

where $\delta(.)$ is the function of Dirac delta. In the above equation, the subsequent approximation is set as a subsequent function which is approximated by N samples set [49].

$$F = \begin{bmatrix} 1 & 0 & 0 \\ 0 & 1 & 0 \\ 0 & 0 & 1 \end{bmatrix}, \tag{32}$$

$$B = \begin{bmatrix} dt.\cos\left(x(3)\right) & 0 \\ dt.\sin\left(x(3)\right) & 0 \\ 0 & dt \end{bmatrix}. \tag{33}$$

As mentioned above in equations (32) and (33), F and B denote the motion and measurement model state transition matrices.

4. Simulation Discussion and Comparison

In the above sections, the authors investigated the localization performance of the proposed EKF, UKF, and PF techniques. Each technique of localization performs well in its context; however, their efficiency differs from one another in some factors. A separate simulation is conducted for each localization technique, but some parameters are consistent through different iterations in these approaches. These parameters include such as those of the first case; the velocity is chosen as $v = 1$ m/s and the time is $T = 10$ sec as presented in Figures 1, 2, and 3, respectively. Table 2 shows the parameters used in the simulations. Furthermore, the initial time is chosen to be $t = 0$ and $t = 60$ sec which represent the end time, while the global time is chosen to be $dt = 0.1$ sec. For navigation, Dead Reckoning (DR) is the method of measuring one's current location by using a previously defined location, using speed and course estimates over time. On the other hand, Ground Truth (GT) is required for real-time localization. The first case state vector is $x_{\text{Est}} = [0 \quad 0 \quad 0]^t$ where the true state can be $x_{\text{Tru}} = x_{\text{Est}}$. At the initial stage, the observation vector is calculated in such way $z = [0 \quad 0 \quad 0 \quad 0]^t$; also, the matrix of covariance Q for motion and covariance matrix for observation R are calculated. While calculating Q and R, the sigma points are calculated. For the PF technique, the function $f_k(x_k)$ is used to calculate the importance of weights w_i. The subsequent approximation $p(x_k \mid z_{1:k})$ and the state estimation $\bar{x}_{k|k}$ are calculated in equations (28) to (31). The Jacobian matrices F of the state equation calculated in equation (32) and Jacobian of motion model JF is calculated in equation (33). The coverage area in all three methods is almost similar, while the localization accuracy is varying. Besides this, the time consumption for all three techniques is dissimilar as can be seen in Table 3 where the velocity and time are reserved constant during four iterations.

In the next step, the velocity v is varied to $v = 2$, $v = 3$, $v = 4$, $v = 5$, $v = 6$, $\cdots$, $v = 10$ m/s. By the variable speed, the coverage range is enlarged as shown in Figures 4 and 5. The velocity variation is considered for the EKF and UKF techniques similarly, but the effect is different in each technique. The coverage of localization in the UKF-based technique is higher (see Figure 5) than the EKF algorithm (see Figure 4). In this phase, the localization coverage is higher, but unfortunately, the localization accuracy is also affected. When the robot is traveling with a higher speed during the process of localization, the mobile robot has a lower communication with the sensors in the surrounding, but if the robot is traveling with a lower speed, the process of communication is more reliable and convenient as compared to the case of high speed. Therefore, the author concludes that the proposed techniques are more accurate and reliable for lower velocities.

Furthermore, the proposed localization techniques' performance is evaluated in different scenarios. The performance is assessed by varying the time of T in all three techniques of localization. However, the velocity is kept constant in all three approaches as can be seen in Table 4. By changing the time T, the localization performance is also varying as can be seen in Figures 6, 7, and 8. In the case of EKF-based localization, by changing the time T, the localization coverage is decreasing as shown in Figure 6. Secondly, in the case of UKF-based localization, by varying the time T, the localization coverage is decreasing as presented in Figure 7. Similarly, by changing the time of T in the PF-based localization, the coverage area is decreasing gradually. It shows that the time T is inverse proportional to the coverage area of localization in all three techniques of localization. However, the time consumption is different in all three techniques as can be seen in Table 4. Among all three localization approaches, PF is the lowest time consumer as compared to other approaches. To compare the time consumption of our proposed PF technique with other techniques, the authors in [50] presented a PF technique Wi-Fi target localization. The technique is used to solve the localization problem of radio source by applying the RSSI measurements. The technique exploits the behavior of wireless signals in free space which obtains the estimates of positions from the signal strength. The authors considered the time-varying strategy to evaluate the performance of localization. The time is enlarged to $T = 1$ sec, $T = 20$ sec, $T = 50$ sec, and $T = 100$ sec, but unfortunately, by increasing the time more and more, the performance is gradually decreasing. However, in our proposed localization techniques, by varying the time T, the performance is still much better as compared to the other techniques.

As mentioned before, every method performs well in its domain, but concerning some aspects, their performance is varying. To compare the proposed methods, the authors evaluated their performance while considering several factors such as localization coverage, time consumption, and localization accuracy. In the PF algorithm,

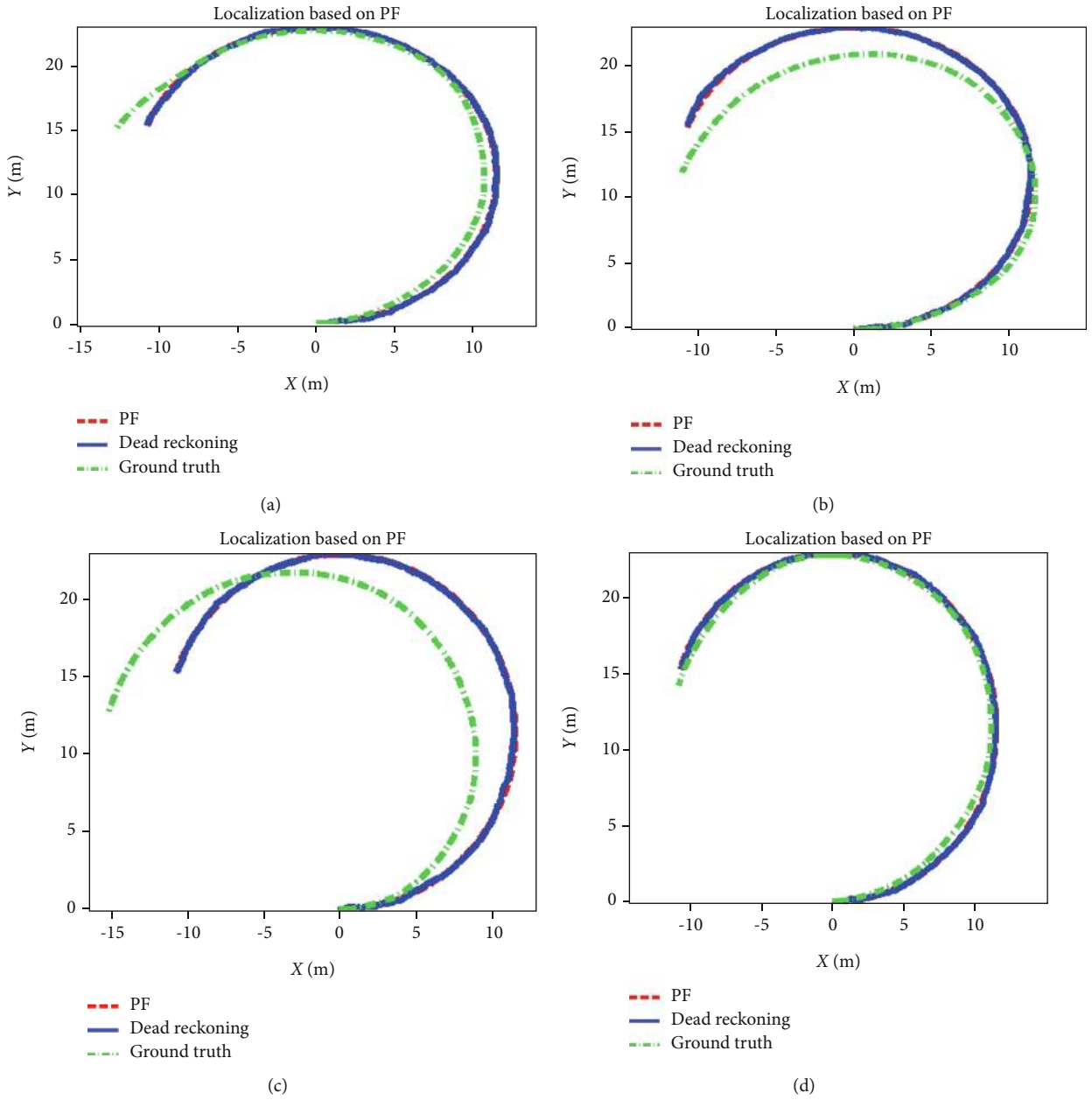

Figure 3: Localization comparison of PF technique. In this phase, for all four iterations, the velocity is $v = 1$ m/s and time is $t = 60$ sec.

the time consumption is lower than in the EKF and UKF algorithms as shown in Table 3. Moreover, UKF is less time consuming as compared to the EKF technique. However, the localization accuracy of EKF and UKF is higher than the PF localization technique. In comparison with other techniques, the performance of the proposed technique is better than the previous as investigated in the literature. A number of localization approaches are presented by the researchers [14, 43, 51, 52]. Each approach focused on the localization performance, but a limited number of aspects are considered such as most of them focused only on the accuracy of localization. However, our proposed methods consider several aspects at once such as the localization coverage, localization accuracy, and consumption of time. Therefore, to the best of the author's knowledge, the proposed techniques are performing well in comparison with other techniques in this field.

5. Conclusion

To conclude, in this paper, the authors addressed three localization strategies based on EKF, UKF, and PF techniques. The authors evaluated the efficiency of the proposed techniques of localization by considering many factors such as the scope of localization, the accuracy of localization, and time of consumption. Basically, two steps are used to investigate the proposed localization techniques. Firstly, the authors kept the velocity of the robot constantly i.e., $v = 1$ m/s, and the process is repeated for four iterations as shown in

Table 2: Parameters used in simulations.

Parameters	Values
Time (T)	10 sec
Initial time (t)	0 sec
Final time (t)	60 sec
Global time (t)	0.1 sec
Initial velocity (v)	1.0 m/s
Updated velocities (v)	1, 2, 3,...,10 m/s
Degree to radian	180°
Yaw rate	5 deg/sec
Sigma points (i)	$i = 1, 2, 3, \cdots, n$
α	0.001
β	2
κ	0
Prediction covariance matrix (Q)	0.1
Observation covariance matrix (Q)	1
N_{eff}	1.0
Total range	360°
Weights (w_i)	$i = 1, 2, 3, \cdots, 2n$

Table 3: Comparison of the time consumption by EKF, UKF, and PF localization techniques.

Velocities	Iterations	Time_{EKF}	Time_{UKF}	Time_{PF}
V1 = 1 m/s	1	6.7431 sec	5.9950 sec	5.5588 sec
	2	6.7009 sec	5.9716 sec	5.5312 sec
	3	6.6051 sec	5.9627 sec	5.5436 sec
	4	6.4641 sec	5.9503 sec	5.5521 sec
V2 = 2 m/s	1	6.3744 sec	5.9005 sec	-
V3 = 3 m/s	1	6.3919 sec	5.9609 sec	-
V4 = 4 m/s	1	6.3835 sec	5.9306 sec	-
V5 = 5 m/s	1	6.1829 sec	5.9171 sec	-
V6 = 6 m/s	1	6.2834 sec	5.7584 sec	-
…	…	…	…	…
V10 = 10 m/s	1	6.2380 sec	5.8450 sec	-

Figures 1, 2, and 3. In the second case, the velocity of the robot is varied to $v = 2$ m/s, $v = 3$ m/s, and so on. As a result, the localization scope often differs by changing the velocity of the robot, as shown in Figure 4 (EKF) and Figure 5 (UKF). Furthermore, the authors evaluated the time consumption of the proposed localization techniques. Among all these techniques, the PF's time consumption is lower compared to the localization techniques of EKF and UKF as shown in Table 2. However, the localization accuracy of EKF and UKF is better than the PF-based localization. Finally, the proposed methods are compared with each other's and also with other standard approaches. Therefore, the proposed localization methods performed better as compared to the other techniques as mentioned in the above section of comparison.

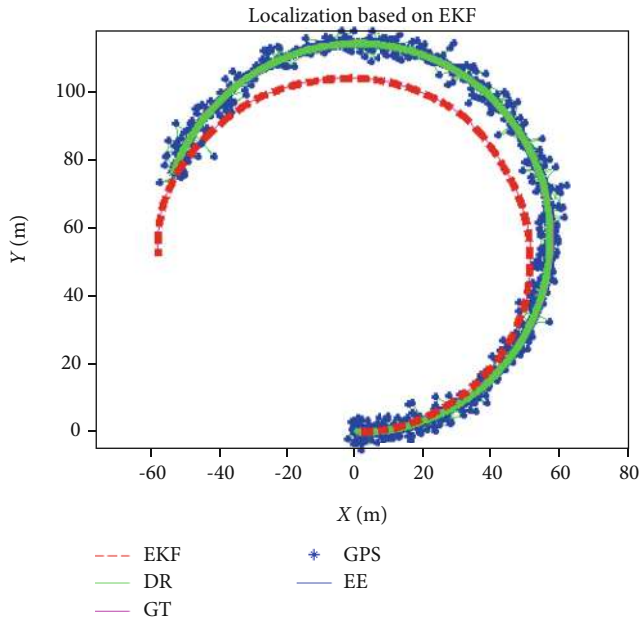

Figure 4: EKF localization with velocity $v = 5$ m/s.

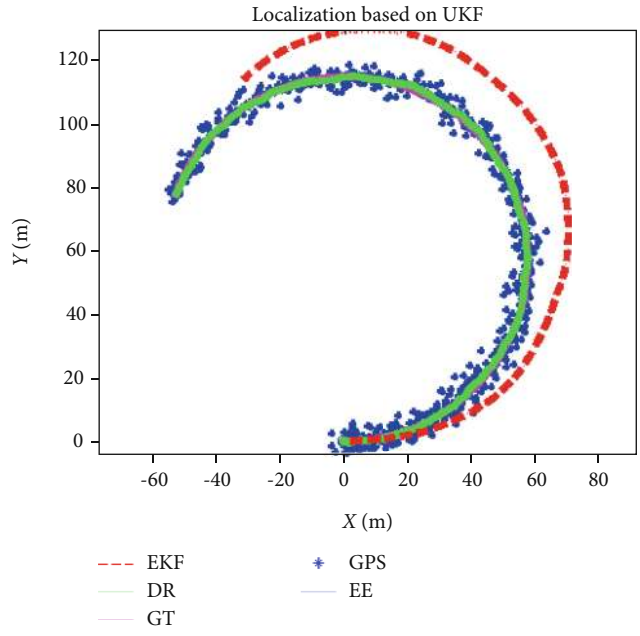

Figure 5: UKF localization with velocity $v = 5$ m/s.

Table 4: Performance comparison of EKF, UKF, and PF localization algorithms by varying the time T.

Time (T)	Velocity (V)	Time_{EKF}	Time_{UKF}	Time_{PF}
$T = 10$ sec	$V = 1$ m/s	6.3845 sec	5.9253 sec	5.5112 sec
$T = 30$ sec	$V = 1$ m/s	6.5245 sec	5.7664 sec	5.3805 sec
$T = 60$ sec	$V = 1$ m/s	6.6377 sec	5.7263 sec	5.7213 sec
$T = 90$ sec	$V = 1$ m/s	6.9117 sec	5.7601 sec	5.1393 sec
$T = 120$ sec	$V = 1$ m/s	6.2887 sec	5.8666 sec	5.2038 sec

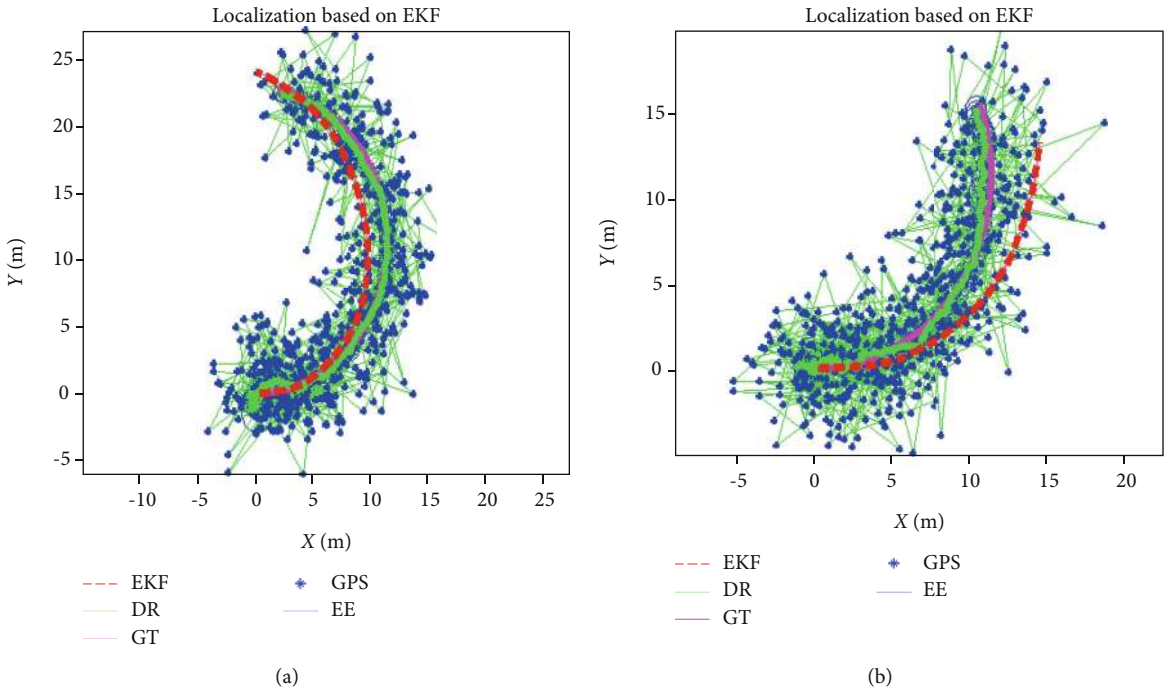

Figure 6: Localization performance of EKF with (a) $T = 30$ sec and (b) $T = 90$ sec.

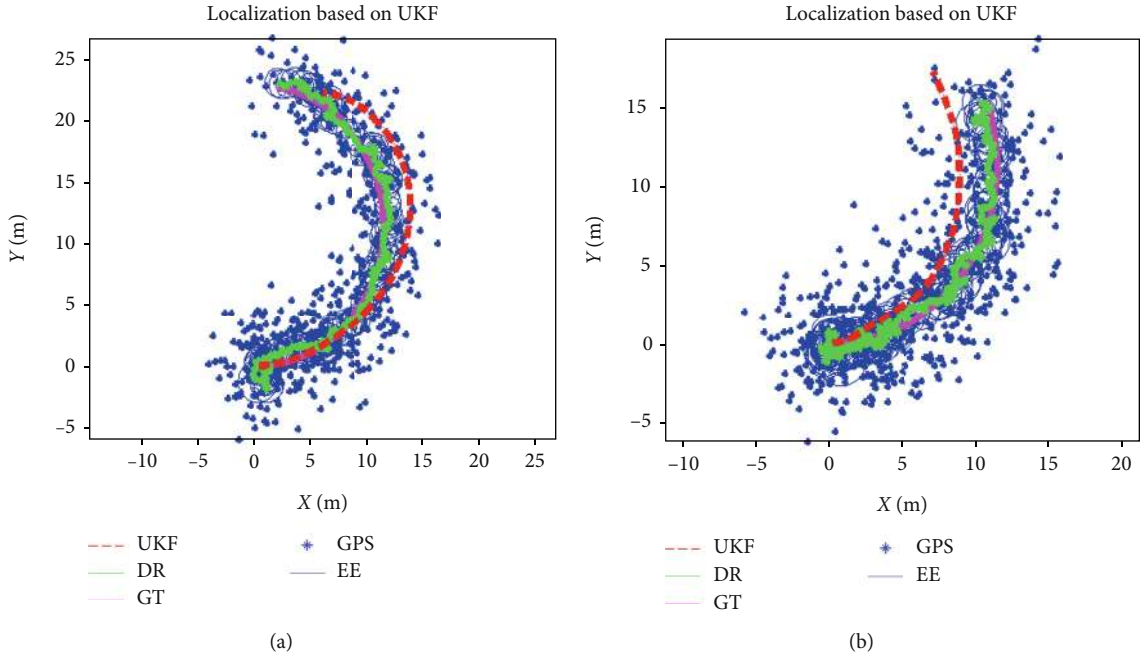

Figure 7: Localization performance of UKF with (a) $T = 30$ sec and (b) $T = 90$ sec.

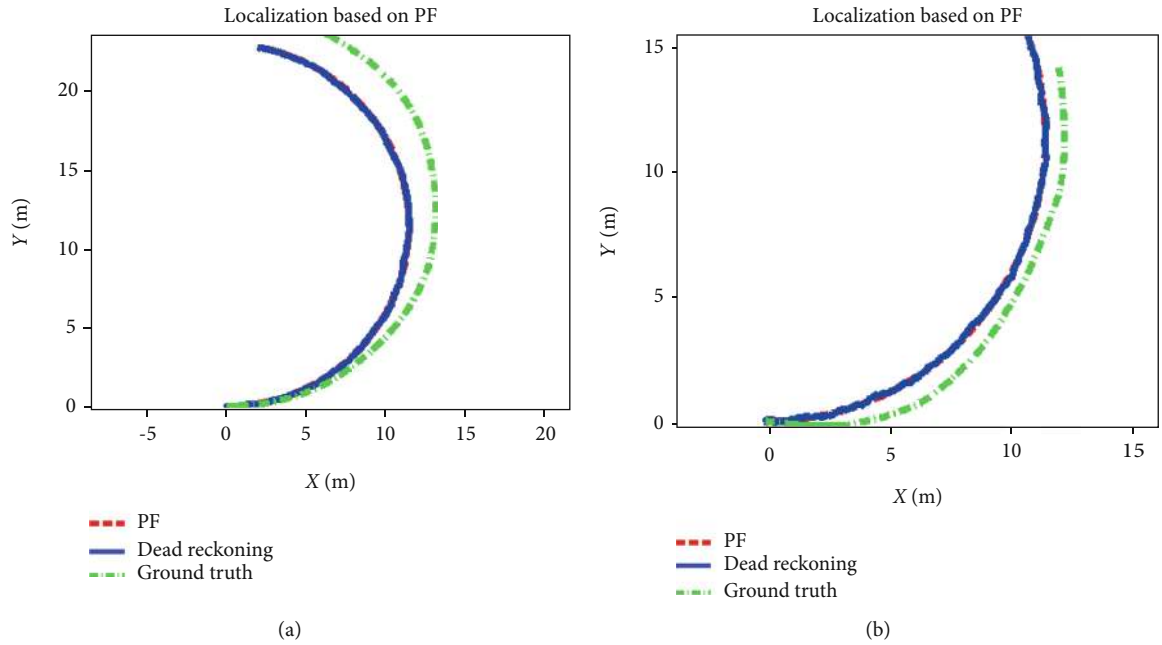

Figure 8: Localization performance of PF with (a) $T = 30$ sec and (b) $T = 90$ sec.

In the future, the authors will perform more experiments to study the effects and performance of these localization methods. In addition, our future study will also have a look on the performance of these localization techniques in combination with the simultaneous robotic localization and mapping.

Data Availability

Since the funding project is not closed and related patents have been evaluated, the simulation data used to support the findings of this study are currently under embargo while the research findings are commercialized. Requests for data, based on the approval of patents after project closure, will be considered by the corresponding author.

Conflicts of Interest

The authors declare that they have no conflicts of interest.

Acknowledgments

This research is supported by the National Key Research and Development Program under Grant 2016YFC0401606 and in part by the National Natural Science Foundation of China under Grant 61671202 and 61801166. It was also supported by the Basic Science Research Program through the National Research Foundation of Korea (NRF) funded by the Ministry of Education under Grant NRF-2018R1D1A1B07043331.

References

[1] R. Khan, S. U. Khan, S. Khan, and M. U. A. Khan, "Localization performance evaluation of extended Kalman filter in wireless sensors network," *Procedia Computer Science*, vol. 32, pp. 117–124, 2014.

[2] I. Ullah, J. Chen, X. Su, C. Esposito, and C. Choi, "Localization and detection of targets in underwater wireless sensor using distance and angle based algorithms," *IEEE Access*, vol. 7, pp. 45693–45704, 2019.

[3] K. Sha, T. A. Yang, W. Wei, and S. Davari, "A survey of edge computing based designs for IoT security," *Digital Communications and Networks*, vol. 6, no. 2, pp. 195–202, 2020.

[4] X. Su, H. Yu, W. Kim, C. Choi, and D. Choi, "Interference cancellation for non-orthogonal multiple access used in future wireless mobile networks," *EURASIP Journal on Wireless Communications and Networking*, vol. 2016, no. 1, 2016.

[5] A. Shareef, Y. Zhu, V. M. Moreno, and A. Pigazo, "Localization using extended Kalman filters in wireless sensor networks," *Kalman Filter Recent Advances and Applications*, pp. 297–320, 2009.

[6] P. Thulasiraman and K. A. White, "Topology control of tactical wireless sensor networks using energy efficient zone routing," *Digital Communications and Networks*, vol. 2, no. 1, pp. 1–14, 2016.

[7] L. Zhu, Y. Li, F. R. Yu, B. Ning, T. Tang, and X. Wang, "Cross-layer defense methods for jamming-resistant CBTC systems," *IEEE Transactions on Intelligent Transportation Systems*, 2020.

[8] I. Ullah, X. Su, X. Zhang, and D. Choi, "Simultaneous localization and mapping based on Kalman filter and extended Kalman filter," *Wireless Communications and Mobile Computing*, vol. 2020, Article ID 2138643, 12 pages, 2020.

[9] W. Yu, J. Peng, X. Zhang, S. Li, and W. Liu, "An adaptive unscented particle filter algorithm through relative entropy for mobile robot self-localization," *Mathematical Problems in Engineering*, vol. 2013, Article ID 567373, 9 pages, 2013.

[10] E. Ivanjko, A. Kitanov, and I. Petrovic, "Model based Kalman filter mobile robot self-localization," *Robot Localization and Map Building*, pp. 59–89, 2010.

[11] S. Safavat, N. N. Sapavath, and D. B. Rawat, "Recent advances in mobile edge computing and content caching," *Digital Communications and Networks*, vol. 6, no. 2, pp. 189–194, 2020.

[12] L. Teslić, I. Škrjanc, and G. Klančar, "EKF-based localization of a wheeled mobile robot in structured environments," *Journal of Intelligent & Robotic Systems*, vol. 62, no. 2, pp. 187–203, 2011.

[13] R. Kandepu, B. Foss, and L. Imsland, "Applying the unscented Kalman filter for nonlinear state estimation," *Journal of Process Control*, vol. 18, no. 7-8, pp. 753–768, 2008.

[14] A. Giannitrapani, N. Ceccarelli, F. Scortecci, and A. Garulli, "Comparison of EKF and UKF for spacecraft localization via angle measurements," *IEEE Transactions on Aerospace and Electronic Systems*, vol. 47, no. 1, pp. 75–84, 2011.

[15] J. M. Pak, C. K. Ahn, P. Shi, Y. S. Shmaliy, and M. T. Lim, "Distributed hybrid particle/fir filtering for mitigating NLOS effects in toa-based localization using wireless sensor networks," *IEEE Transactions on Industrial Electronics*, vol. 64, no. 6, pp. 5182–5191, 2017.

[16] I. Ullah, Y. Liu, X. Su, and P. Kim, "Efficient and accurate target localization in underwater environment," *IEEE Access*, vol. 7, pp. 101415–101426, 2019.

[17] W. R. Gilks and C. Berzuini, "Following a moving target-Monte Carlo inference for dynamic Bayesian models," *Journal of the Royal Statistical Society: Series B (Statistical Methodology)*, vol. 63, no. 1, pp. 127–146, 2001.

[18] J. M. Pak, C. K. Ahn, Y. S. Shmaliy, and M. T. Lim, "Improving reliability of particle filter-based localization in wireless sensor networks via hybrid particle/fir filtering," *IEEE Transactions on Industrial Informatics*, vol. 11, no. 5, pp. 1089–1098, 2015.

[19] C. K. Ahn, P. Shi, and M. V. Basin, "Deadbeat dissipative fir filtering," *IEEE Transactions on Circuits and Systems I: Regular Papers*, vol. 63, no. 8, pp. 1210–1221, 2016.

[20] M. Raja, "Application of cognitive radio and interference cancellation in the L-band based on future air-to-ground communication systems," *Digital Communications and Networks*, vol. 5, no. 2, pp. 111–120, 2019.

[21] C. K. Ahn, "Strictly passive FIR filtering for state-space models with external disturbance," *AEU-International Journal of Electronics and Communications*, vol. 66, no. 11, pp. 944–948, 2012.

[22] J. M. Pak, S. Y. Yoo, M. T. Lim, and M. K. Song, "Weighted average extended FIR filter bank to manage the horizon size in nonlinear fir filtering," *International Journal of Control, Automation and Systems*, vol. 13, no. 1, pp. 138–145, 2015.

[23] P. M. Pradhan and G. Panda, "S-transformation based integrated approach for spectrum estimation, storage, and sensing in cognitive radio," *Digital Communications and Networks*, vol. 5, no. 3, pp. 160–169, 2019.

[24] J. M. Pak, C. K. Ahn, Y. S. Shmaliy, P. Shi, and M. T. Lim, "Switching extensible fir filter bank for adaptive horizon state estimation with application," *IEEE Transactions on Control Systems Technology*, vol. 24, no. 3, pp. 1052–1058, 2016.

[25] Y. Li, S. Xia, B. Cao, and Q. Liu, "Lyapunov optimization based trade-off policy for mobile cloud offloading in heterogeneous wireless networks," *IEEE Transactions on Cloud Computing*, 2019.

[26] W. Cui, B. Li, L. Zhang, and W. Meng, "Robust mobile location estimation in NLOS environment using GMM, IMM, and EKF," *IEEE Systems Journal*, vol. 13, no. 3, pp. 3490–3500, 2018.

[27] T.-J. Ho, "Robust urban wireless localization: synergy between data fusion, modeling and intelligent estimation," *IEEE Transactions on Wireless Communications*, vol. 14, no. 2, pp. 685–697, 2014.

[28] M. Lipka, E. Sippel, and M. Vossiek, "An extended Kalman filter for direct, real-time, phase-based high precision indoor localization," *IEEE Access*, vol. 7, pp. 25288–25297, 2019.

[29] L. Zhu, Y. He, F. R. Yu, B. Ning, T. Tang, and N. Zhao, "Communication-based train control system performance optimization using deep reinforcement learning," *IEEE Transactions on Vehicular Technology*, vol. 66, no. 12, pp. 10705–10717, 2017.

[30] K. Lee, J. Oh, and K. You, "TDOA-/FDOA-based adaptive active target localization using iterated dual-EKF algorithm," *IEEE Communications Letters*, vol. 23, no. 4, pp. 752–755, 2019.

[31] X. Su, I. Ullah, X. Liu, and D. Choi, "A review of underwater localization techniques, algorithms, and challenges," *Journal of Sensors*, vol. 2020, Article ID 6403161, 24 pages, 2020.

[32] Y. Li, J. Liu, B. Cao, and C. Wang, "Joint optimization of radio and virtual machine resources with uncertain user demands in mobile cloud computing," *IEEE Transactions on Multimedia*, vol. 20, no. 9, pp. 2427–2438, 2018.

[33] Y. Wang, H. Jie, and L. Cheng, "A fusion localization method based on a robust extended Kalman filter and track-quality for wireless sensor networks," *Sensors*, vol. 19, no. 17, p. 3638, 2019.

[34] C.-D. Wann, Y.-J. Yeh, and C.-S. Hsueh, "Hybrid TDOA/AOA indoor positioning and tracking using extended Kalman filters," in *2006 IEEE 63rd Vehicular Technology Conference*, pp. 1058–1062, Melbourne, Vic., Australia, May 2006.

[35] X. Su, K. Fan, and W. Shi, "Privacy-preserving distributed data fusion based on attribute protection," *IEEE Transactions on Industrial Informatics*, vol. 15, no. 10, pp. 5765–5777, 2019.

[36] X. Ou, X. Wu, X. He, Z. Chen, and Q.-A. Yu, "An improved node localization based on adaptive iterated unscented Kalman filter for WSN," in *2015 IEEE 10th Conference on Industrial Electronics and Applications (ICIEA)*, pp. 393–398, Auckland, New Zealand, June 2015.

[37] P. Del Moral, A. Doucet, and A. Jasra, "An adaptive sequential Monte Carlo method for approximate Bayesian computation," *Statistics and Computing*, vol. 22, no. 5, pp. 1009–1020, 2012.

[38] L. Mihaylova, A. Y. Carmi, F. Septier, A. Gning, S. K. Pang, and S. Godsill, "Overview of bayesian sequential Monte Carlo methods for group and extended object tracking," *Digital Signal Processing*, vol. 25, pp. 1–16, 2014.

[39] S. J. Julier and J. K. Uhlmann, "Unscented filtering and nonlinear estimation," *Proceedings of the IEEE*, vol. 92, no. 3, pp. 401–422, 2004.

[40] J. Hammersley, *Monte Carlo Methods*, Springer Science & Business Media, 2013.

[41] S. Kluge, K. Reif, and M. Brokate, "Stochastic stability of the extended Kalman filter with intermittent observations," *IEEE Transactions on Automatic Control*, vol. 55, no. 2, pp. 514–518, 2010.

[42] L. Zhu, F. R. Yu, B. Ning, and T. Tang, "Cross-layer handoff design in MIMO-enabled WLANs for communication-based train control (CBTC) systems," *IEEE Journal on Selected Areas in Communications*, vol. 30, no. 4, pp. 719–728, 2012.

[43] L. D. Alfonso, A. Grano, P. Muraca, and P. Pugliese, "Extended and unscented Kalman filters in a cells-covering method for environment reconstruction," in *2019 IEEE 15th International Conference on Control and Automation (ICCA)*, pp. 1557–1562, Edinburgh, United Kingdom, United Kingdom, July 2019.

[44] M. Moreno-Cano, M. A. Zamora-Izquierdo, J. Santa, and A. F. Skarmeta, "An indoor localization system based on artificial

neural networks and particle filters applied to intelligent buildings," *Neurocomputing*, vol. 122, pp. 116–125, 2013.

[45] D. Fox, "Kld-sampling: adaptive particle filters," in *Advances in Neural Information Processing Systems: Natural and Synthetic*, Vancouver, British Columbia, Canada, December 3-8, 2001.

[46] C.-H. Park and J.-H. Chang, "Robust LMedS-based WLS and Tukey-based EKF algorithms under LOS/NLOS mixture conditions," *IEEE Access*, vol. 7, pp. 148198–148207, 2019.

[47] B. T. Burchett, "Unscented Kalman filters for range-only cooperative localization of swarms of munitions in three-dimensional flight," *Aerospace Science and Technology*, vol. 85, pp. 259–269, 2019.

[48] I. Ullah, Y. Shen, X. Su, C. Esposito, and C. Choi, "A localization based on unscented Kalman filter and particle filter localization algorithms," *IEEE Access*, vol. 8, pp. 2233–2246, 2019.

[49] B.-F. Wu and C.-L. Jen, "Particle-filter-based radio localization for mobile robots in the environments with low-density wlan aps," *IEEE Transactions on Industrial Electronics*, vol. 61, no. 12, pp. 6860–6870, 2014.

[50] N. Wagle and E. Frew, "A particle filter approach to wifi target localization," in *AIAA guidance, navigation, and control conference*, p. 7750, Toronto, Ontario, Canada, August 2010.

[51] C. Yang, W. Shi, and W. Chen, "Comparison of unscented and extended Kalman filters with application in vehicle navigation," *The Journal of Navigation*, vol. 70, no. 2, pp. 411–431, 2017.

[52] K. Ahn and Y. Kang, "A particle filter localization method using 2d laser sensor measurements and road features for autonomous vehicle," *Journal of Advanced Transportation*, vol. 2019, Article ID 3680181, 11 pages, 2019.